THE SIX ELECTROMAGNETIC FIELD COMPONENTS AT LOW FREQUENCY IN AN AXISYMMETRIC INFINITELY THICK SINGLE-LAYER RESISTIVE BEAM PIPE

N. Mounet (EPFL, Lausanne and CERN, Geneva) and E. Métral (CERN, Geneva)

Abstract

In this study B. Zotter's formalism is applied to a circular infinitely long beam pipe made of a conductor of infinite thickness where an offset point-charge travels at any given speed. Simple formulae are found for the impedances and electromagnetic fields both at intermediate frequencies (recovering Chao's results) and in the low frequency regime where the usual classic thick wall impedance formula does not apply anymore due to the large skin depth compared to the pipe radius.

INTRODUCTION

In the LHC, the beam-coupling impedance coming from graphite collimators deviates significantly [1] from the classic thick wall formula [2, p. 71] at low frequency, due the large skin depth in graphite that becomes comparable or even larger than the half gap. At such low frequencies the impedance of the collimators can be computed analytically thanks to the more general formalism of B. Zotter [3, 4], but we still lack a complete analysis of the behaviour of the electromagnetic (EM) field components. In particular in this new frequency regime it is crucial to know theoretically if some approximations made in bench measurements [1] are still valid.

Zotter's formalism gives in principle analytical expressions of the EM fields [5], but formulae are complicated and the relevant physical parameters difficult to identify. We will use here this formalism to find new approximations of the electromagnetic fields and impedances at low and intermediate frequencies that will be easier to understand, in the case of an infinitely thick cylindrical beam pipe made of a relatively good conductor. Derivations of the formulae shown below will be detailed in a later publication [6].

ELECTROMAGNETIC CONFIGURATION

We consider the electromagnetic problem of [5], i.e. a point-like beam of charge Q travelling at a speed $v = \beta c$ along the axis of an axisymmetric infinitely long pipe of inner radius b, at the position $(r = a, \theta = 0, s = vt)$ in cylindrical coordinates. The pipe is made of one infinitely thick single layer as shown in Fig. 1. Only the two first azimuthal modes $m = 0$ and 1 are considered, as the other ones have a low impact on the EM forces near the center of the pipe [6]. The source charge density is in frequency domain ($f = \frac{\omega}{2\pi}$) [7]

$$\rho_m = \frac{Q\cos(m\theta)\delta(r-a)e^{-jks}}{\pi v a(1+\delta_{m0})}, \qquad (1)$$

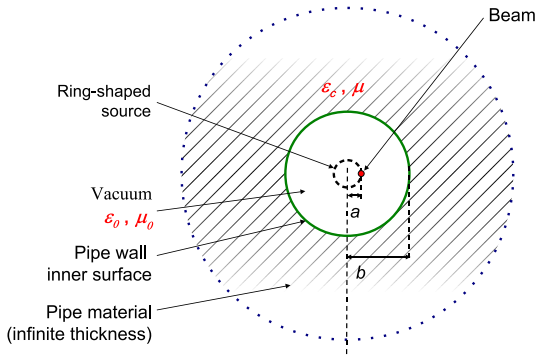

Figure 1: Cross section of the pipe.

where $k \equiv \frac{\omega}{v}$, δ is the Dirac distribution, and $\delta_{m0} = 1$ if $m = 0$, 0 otherwise. We take for the complex permittivity and permeability inside the pipe wall [1]

$$\varepsilon_c = \varepsilon_0\varepsilon_1 = \varepsilon_0\varepsilon_b + \frac{\sigma_{DC}}{j\omega\,(1+j\omega\tau)}, \quad \mu = \mu_0\mu_r.$$

In these expressions, ε_0 (μ_0) is the permittivity (permeability) of vacuum, ε_b the real dielectric constant, μ_r the relative permeability, σ_{DC} the DC conductivity and τ the relaxation time. We use the Drude model [8, p. 312] for the AC conductivity, and assume the validity of local Ohm's law. In the following $\vec{E}$ and $\vec{H}$ are the electric and magnetic fields, $\vec{G} = Z_0 H$ where $Z_0 = \mu_0 c$ is the free space impedance, and all frequencies are taken positive.

GENERAL APPROXIMATIONS FOR THE EM FIELDS IN FREQUENCY DOMAIN

Using the exact formulae of the EM fields from [5], taking away the direct space-charge part (i.e. the fields created by the source if no pipe were present), we can approximate the remaining "wall" [1] part of the fields components in the vacuum region under some conditions detailed in Table 1 [6]. For $m = 0$ we get (with $\gamma^{-2} = 1 - \beta^2$)

$$E_s^{W_0} \approx -\frac{j\omega Q e^{-jks}}{2\pi\varepsilon_0 v^2\gamma^2}\left[\frac{K_0(x_1)}{I_0(x_1)} - \frac{1}{x_1^2 f(x_2)}\right], \qquad (2)$$

$$E_r^{W_0} \approx \frac{\omega Q u_1 e^{-jks}}{4\pi\varepsilon_0 v^2\gamma}\left[\frac{K_0(x_1)}{I_0(x_1)} - \frac{1}{x_1^2 f(x_2)}\right], \qquad (3)$$

$$G_\theta^{W_0} = \beta E_r^{W_0}, \quad G_s^{W_0} = G_r^{W_0} = E_\theta^{W_0} = 0, \qquad (4)$$

and for $m = 1$

$$\frac{E_s^{W_1}}{\tilde{E}_s^{W_1}} = \frac{E_r^{W_1}}{\tilde{E}_r^{W_1}} = \frac{G_\theta^{W_1}}{\tilde{G}_\theta^{W_1}} = Q\cos\theta e^{-jks}, \qquad (5)$$

Table 1: Conditions for Eqs. (2) to (12) to be valid, with numerical values for the bounds (in rad/s) in two cases: stainless steel beam pipe at low energy ($b = 8$ cm, $\sigma_{DC} = 10^6$ S/m, $\tau = 0$, $\gamma = 1.05$) and LHC graphite collimator ($b = 2$ mm, $\sigma_{DC} = 10^5$ S/m, $\tau = 0.8$ ps, $\gamma = 7.46 \cdot 10^3$). In both cases $\varepsilon_b = \mu_r = 1$.

Conditions	Low γ, ss pipe	LHC coll.
$\lvert\omega\rvert\tau \ll 1$	No bound	$1.3 \cdot 10^{12}$
$\lvert\omega\rvert \ll \frac{1}{\varepsilon_0}\frac{\beta^2\mu_r\sigma_{DC}}{1-\beta^2\mu_r\varepsilon_b}$	$1.2 \cdot 10^{16}$	$6.3 \cdot 10^{23}$
$\lvert\omega\rvert \ll \frac{\beta\gamma c}{b}$	$1.2 \cdot 10^{9}$	$1.1 \cdot 10^{15}$
$\lvert\omega\rvert \ll \left[\frac{v^4\gamma^4\mu_0\sigma_{DC}}{b^2\mu_r}\right]^{\frac{1}{3}}$	$2.6 \cdot 10^{11}$	$9.2 \cdot 10^{17}$
$\lvert\omega\rvert \ll \frac{\sigma_{DC}}{\varepsilon_b\varepsilon_0}$	$1.1 \cdot 10^{17}$	$1.1 \cdot 10^{16}$
$\lvert\omega\rvert \ll \frac{\beta^2\gamma\sigma_{DC}}{\varepsilon_0}$	$1.1 \cdot 10^{16}$	$8.4 \cdot 10^{19}$
$\lvert\omega\rvert \ll \frac{\beta^2\mu_r\sigma_{DC}}{\varepsilon_0}$	$1.1 \cdot 10^{16}$	$1.1 \cdot 10^{16}$
$\lvert\omega\rvert \ll \frac{\beta^2\sigma_{DC}}{\mu_r\varepsilon_0}$	$1.1 \cdot 10^{16}$	$1.1 \cdot 10^{16}$
$\lvert\omega\rvert \ll \left[\frac{8v^4\mu_0\sigma_{DC}}{b^2(1+\beta^2)^2\mu_r}\right]^{\frac{1}{3}}$	$4.5 \cdot 10^{11}$	$8 \cdot 10^{12}$
$\lvert\omega\rvert \ll \frac{v^4\mu_r(\mu_0\sigma_{DC})^3b^2}{8}$	$1.1 \cdot 10^{29}$	$8 \cdot 10^{24}$

$$\frac{G_s^{W_1}}{\tilde{G}_s^{W_1}} = \frac{G_r^{W_1}}{\tilde{G}_r^{W_1}} = \frac{E_\theta^{W_1}}{\tilde{E}_\theta^{W_1}} = Q\sin\theta e^{-jks}, \tag{6}$$

$$\tilde{E}_s^{W_1} \approx \frac{-j\omega\mu_0 x_0 u_1}{4\pi\beta^2\gamma^2}\left[\frac{K_1(x_1)}{I_1(x_1)} + \frac{4\beta^2\gamma^2}{x_1^2 g(x_2)}\right], \tag{7}$$

$$\tilde{G}_s^{W_1} \approx \frac{j\omega\mu_0 x_0 u_1}{\pi\beta x_1^2}\frac{1-x_1^2 h(x_2)}{g(x_2)}, \tag{8}$$

$$\tilde{E}_r^{W_1} \approx \frac{\omega\mu_0 x_0}{4\pi\beta^2\gamma}\left[\frac{K_1(x_1)}{I_1(x_1)} + \frac{4\beta^2\gamma^2\left(h(x_2)+\frac{u_1^2}{4x_1^2}\right)}{g(x_2)}\right], \tag{9}$$

$$\tilde{E}_\theta^{W_1} \approx \frac{-\omega\mu_0 x_0}{4\pi\beta^2\gamma}\left[\frac{K_1(x_1)}{I_1(x_1)} + \frac{4\beta^2\gamma^2\left(h(x_2)-\frac{u_1^2}{4x_1^2}\right)}{g(x_2)}\right], \tag{10}$$

$$\tilde{G}_r^{W_1} \approx \frac{\omega\mu_0 x_0}{4\pi\beta\gamma}\left[\frac{K_1(x_1)}{I_1(x_1)} - \frac{4-4\gamma^2 x_1^2 h(x_2)+\gamma^2 u_1^2}{x_1^2 g(x_2)}\right], \tag{11}$$

$$\tilde{G}_\theta^{W_1} \approx \frac{\omega\mu_0 x_0}{4\pi\beta\gamma}\left[\frac{K_1(x_1)}{I_1(x_1)} - \frac{4-4\gamma^2 x_1^2 h(x_2)-\gamma^2 u_1^2}{x_1^2 g(x_2)}\right], \tag{12}$$

I_m and K_m being the modified Bessel functions, and with

$$f(x_2) = \frac{1}{2} - \frac{\varepsilon_1}{x_2}\frac{K_0'(x_2)}{K_0(x_2)}, \quad g(x_2) = 1 - \frac{x_2}{\mu_r}\frac{K_1'(x_2)}{K_1(x_2)},$$
$$h(x_2) = \frac{1}{x_2^2} + \frac{1}{4} - \frac{\mu_r}{x_2}\frac{K_1'(x_2)}{K_1(x_2)}, \quad \nu = k\sqrt{1-\beta^2\varepsilon_1\mu_r},$$
$$x_0 = \frac{ka}{\gamma},\ x_1 = \frac{kb}{\gamma},\ x_2 = \nu b,\ u_1 = \frac{kr}{\gamma},\ u_2 = \nu r.$$

As can be seen in Table 1 for two very different cases, those approximations have a broad range of validity even for a poor conductor or at low energy. In Fig. 2 we have plotted the EM field components in vacuum versus frequency for an LHC round collimator.

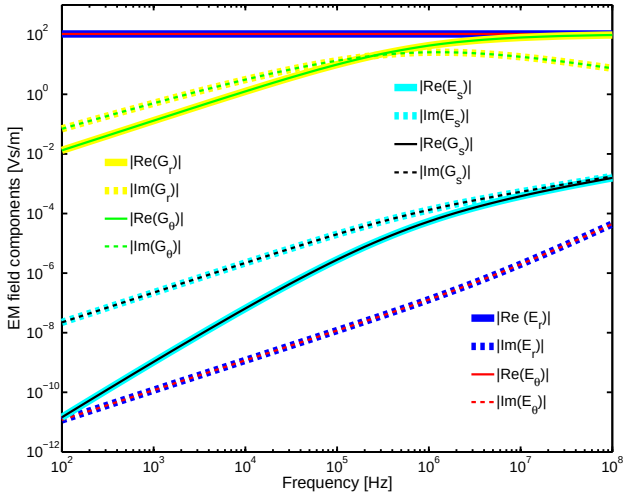

Figure 2: EM fields vs. frequency at $r = 0.1$ mm and $\theta = \frac{\pi}{4}$ for $m = 1$ in a graphite tube (see parameters in Table 1). Beam parameters are $\gamma = 479.7$, $Q = 1$ C and $a = 10\,\mu$m.

Under the same approximations the longitudinal and transverse dipolar wall impedances as defined in [1] (the latter being as usual normalized by the source transverse offset a) are [1, 6]:

$$Z_\parallel^W \approx \frac{j\omega\mu_0 L}{2\pi\beta^2\gamma^2}\left[\frac{K_0(x_1)}{I_0(x_1)} - \frac{1}{x_1^2\left(\frac{1}{2} - \frac{\varepsilon_1}{x_2}\frac{K_0'(x_2)}{K_0(x_2)}\right)}\right], \tag{13}$$

$$Z_x^{W,dip} \approx \frac{jk^2 Z_0 L}{4\pi\beta\gamma^4}\left[\frac{K_1(x_1)}{I_1(x_1)} + \frac{4\beta^2\gamma^2}{x_1^2\left(1 - \frac{x_2}{\mu_r}\frac{K_1'(x_2)}{K_1(x_2)}\right)}\right]. \tag{14}$$

Equation (14) is compared to the exact single-layer impedance [4] in Fig. 3, with the parameters of an LHC round collimator, showing a very good agreement up to several GHz. It is seen that the dipolar transverse impedance shows three different behaviours (which is also true for the longitudinal impedance [4]): one at high frequencies which is not covered by the approximate formulae shown here, one at intermediate frequencies and the last one at low frequencies [1]. Between the two latter the real part of the impedance has a maximum given by [6]:

$$f_{max} \approx \frac{1.986}{\pi b^2\sigma_{DC}\mu_0},\ \mathrm{Re}\left[Z_x^{W,dip}\right]_{max} \approx 0.122\frac{\beta L Z_0}{\pi b^2}, \tag{15}$$

when $\mu_r = 1$. Its value over L depends only on b and β.

INTERMEDIATE FREQUENCIES

From now on we focus on the $m = 1$ mode. When the skin depth $\delta_s = \sqrt{\frac{2}{\mu_0\mu_r\sigma_{DC}\omega}}$ is much smaller than b, we

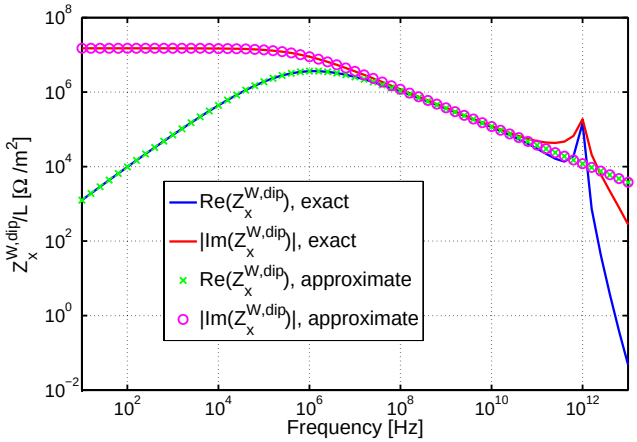

Figure 3: Transverse dipolar impedance (over L) in a graphite tube (parameters of Fig. 2): exact formula [4] and Eq. (14).

can separate the perfect conductor part of the fields from the resistive part. The latter reads [6]

$$\begin{aligned}
\tilde{E}_s^{RW_1} &\approx -\frac{(1+j)ar\sqrt{\omega}\sqrt{\mu_0\mu_r}}{\pi b^3\sqrt{2\sigma}},\\
\tilde{G}_s^{RW_1} &\approx \frac{(1+j)ar\sqrt{\omega}\sqrt{\mu_0\mu_r}}{\pi\beta b^3\sqrt{2\sigma}},\\
\tilde{E}_r^{RW_1} &\approx \frac{(1-j)a\omega^{\frac{3}{2}}\sqrt{\mu_0\mu_r}}{4\pi b^3\sqrt{2\sigma}\upsilon}\left(r^2+b^2\right),\\
\tilde{E}_\theta^{RW_1} &\approx \frac{(1-j)a\omega^{\frac{3}{2}}\sqrt{\mu_0\mu_r}}{4\pi b^3\sqrt{2\sigma}\upsilon}\left(r^2-b^2\right),\\
\tilde{G}_r^{RW_1} &\approx \frac{(-1+j)a\sqrt{\mu_r}}{\pi\beta b^3\sqrt{2\sigma\omega\mu_0}}\left[\beta Z_0+\frac{\omega^2\mu_0\left(r^2-b^2\right)}{4\upsilon}\right],\\
\tilde{G}_\theta^{RW_1} &\approx \frac{(1-j)a\sqrt{\mu_r}}{\pi\beta b^3\sqrt{2\sigma\omega\mu_0}}\left[-\beta Z_0+\frac{\omega^2\mu_0\left(r^2+b^2\right)}{4\upsilon}\right].
\end{aligned} \tag{16}$$

These are in agreement with Chao's formulae [2, p. 52] when $\mu_r = \beta = 1$. The electric field transverse components are much smaller than the magnetic ones: since the second term in G_r is much smaller than the first one, we find for instance $\frac{|\tilde{E}_\theta^{RW_1}|}{|\tilde{G}_r^{RW_1}|} \approx \frac{\omega^2\left(r^2-b^2\right)}{4\beta c^2} \ll 1$ with reasonable parameters. This validates transverse impedance measurements with a coil where only $\vec{G}$ is measured [1].

LOW FREQUENCIES

When $\delta_s \gg b$, it is better to keep the perfect conductor part of the fields with the resistive part because they combine together, which is why the concept of "wall" impedances was introduced [1]. Setting $\mu_r = 1$ here, we get for the "wall" fields in the vacuum region [6]:

$$\begin{aligned}
\tilde{E}_s^{W_1} &\approx \left[\frac{\sigma_{DC}\mu_0^2\omega^2}{4\pi}\ln\left(\frac{be^{\gamma_e}}{\sqrt{2}\delta_s}\right)-\frac{j\mu_0\omega}{2\pi\beta^2b^2}\right]ar,\\
\tilde{G}_s^{W_1} &\approx \left[-\frac{\sigma_{DC}\mu_0^2\omega^2}{4\pi\beta}\ln\left(\frac{be^{\gamma_e}}{\sqrt{2}\delta_s}\right)+\frac{j\mu_0\omega}{2\pi\beta b^2}\right]ar,
\end{aligned}$$

$$\begin{aligned}
\tilde{E}_r^{W_1} &\approx \left[\frac{Z_0}{2\pi\beta b^2}+\frac{\omega^2\mu_0}{2\pi\upsilon}\left(\frac{1}{4}+\frac{r^2}{4b^2}\right)-\frac{j\omega}{\pi\upsilon b^2\sigma_{DC}}\right]a,\\
\tilde{E}_\theta^{W_1} &\approx \left[\frac{-Z_0}{2\pi\beta b^2}+\frac{-\omega^2\mu_0}{2\pi\upsilon}\left(\frac{1}{4}-\frac{r^2}{4b^2}\right)+\frac{j\omega}{\pi\upsilon b^2\sigma_{DC}}\right]a,\\
\tilde{G}_r^{W_1} &\approx \left[\frac{Z_0}{8\delta_s^2}+\frac{\omega^2\mu_0}{2\pi\beta\upsilon}\left(\frac{1}{4}-\frac{r^2}{4b^2}\right)-j\frac{Z_0}{2\pi\delta_s^2}\ln\left(\frac{be^{\gamma_e}}{\sqrt{2}\delta_s}\right)\right]a,\\
\tilde{G}_\theta^{W_1} &\approx \left[\frac{Z_0}{8\delta_s^2}+\frac{\omega^2\mu_0}{2\pi\beta\upsilon}\left(\frac{1}{4}+\frac{r^2}{4b^2}\right)-j\frac{Z_0}{2\pi\delta_s^2}\ln\left(\frac{be^{\gamma_e}}{\sqrt{2}\delta_s}\right)\right]a,
\end{aligned} \tag{17}$$

where $\gamma_e \approx 0.5772$ is Euler's constant. Here the ratio between the imaginary parts of e.g. $\tilde{E}_\theta$ and $\tilde{G}_r$ is $\frac{4}{\beta(bZ_0\sigma_{DC})^2\ln\left(\frac{be^{\gamma_e}}{\sqrt{2}\delta_s}\right)} \ll 1$, but for the real part, taking the first and dominant terms only, we get $\frac{4\delta_s^2}{\pi\beta b^2} \gg 1$. Therefore the imaginary part of $\vec{E}$ is negligible but not its real part, so coil measurements of the impedance will give access only to its real part and not its imaginary part. This is also intuitive as at low frequencies, the EM fields will be mainly due to the electric images sitting at $r = b$, as already discussed in [1].

The transverse dipolar impedance is then given by [1]

$$Z_x^{W,dip} \approx \frac{jLZ_0}{2\pi b^2\beta}-\frac{LZ_0\beta}{2\pi\delta_s^2}\ln\left(\frac{be^{\gamma_e}}{\sqrt{2}\delta_s}\right), \tag{18}$$

in which we see that the skin depth, which characterizes the distance between the image currents and the beam, is the dominant parameter in the real part of the impedance and "replaces" the usual dependence in b.

CONCLUSION

Using Zotter's formalism, the electromagnetic fields created by a beam in a single-layer cylindrical structure have been approximated in frequency domain. New simple expressions were found at low frequencies, where the fields exhibit quite a different behaviour from the one at intermediate frequencies. In a later publication [6], the EM fields in the pipe wall will also be given.

REFERENCES

[1] F. Roncarolo et al, Phys. Rev. ST AB 12 (2009) 084401.
[2] A. W. Chao, "Physics of Collective Beams Instabilities in High Energy Accelerators", John Wiley and Sons (1993).
[3] B. Zotter, CERN-AB-2005-043 (2005).
[4] E. Métral et al, PAC'07, Albuquerque, USA.
[5] N. Mounet and E. Métral, these proceedings.
[6] N. Mounet and E. Métral, CERN note, to be published.
[7] R. L. Gluckstern, CERN-2000-011 (2000).
[8] J. D. Jackson, "Classical Electrodynamics", John Wiley and Sons, 3rd ed (1998).